View metadata, citation and similar papers at core.ac.uk
brought to you by CORE
provided by The University of Utah: J. Willard Marriott Digital Library

A High-Resolution Flexible Tactile Imager System Based on Floating Comb Electrodes

Rajesh Surapaneni, Yan Xie, Qingbo Guo, Darrin J. Young and Carlos H. Mastrangelo
Electrical and Computer Engineering
The University of Utah
Salt Lake City, UT, USA
Rajesh.surapaneni@utah.edu

***Abstract*— Flexible high-resolution contact force imagers are needed in many applications for robotic grippers and gait analysis, but its intrinsic intimate contact requirement often causes breaking of top metallization layers and failure in a short time. The use of floating electrodes has significantly improved the reliability of traditional quad-cell capacitive tactile sensing devices. In this paper we present a new type of high-resolution (676-sensors) flexible pressure/shear imager array based on *floating combs*. Each sensing cell consists of two sets of orthogonal comb electrodes connected in a differential capacitance configuration. The shear sense direction *(+x, -x, +y, -y)* is determined by the amount of asymmetric comb overlap. Pressure readouts are obtained from the net capacitance of the cell. The new comb configuration multiplies the shear capacitive signal by the number of combs per cell. The imager is read using a high-speed switched-capacitor circuit with a 12-bit resolution at full frame rates of 100 Hz (~ 0.8Mb/s).**

I. INTRODUCTION

Flexible tactile imagers (FTIs) that can withstand millions of large deformation cycles are needed in many harsh "rubber-meets-ground" type applications such as robotic grippers and gait analysis [1]. These sensors provide 3-axis tactile measurement in the form of pressure and two-dimensional shear information. For instance, in robotic grippers the shear information is used to detect and correct slippage. In gait analysis, these imagers provide pressure and shear information needed to customize correctional aids.

Durable FTIs are generally difficult to fabricate because periodic deformation during wear can break its vital components such as metal interconnects after just a few hundred or thousands of cycles. The fabrication of reliable FTIs remains an open research problem. The utilization of floating electrodes on top of the deformable dielectric material in the sensor [2-3] significantly reduces failures from emergence of metal breaks as the capacitance readout is completely insensitive to the floating metal connectivity. This is illustrated in the capacitive sensing schemes shown in Fig. 1. In the two-electrode capacitive sensor scheme of Fig. 1(a), a crack on the top conductive drive line directly breaks the electrical circuit, thus disconnecting the sensor from the external readout circuit. In contrast in the floating electrode

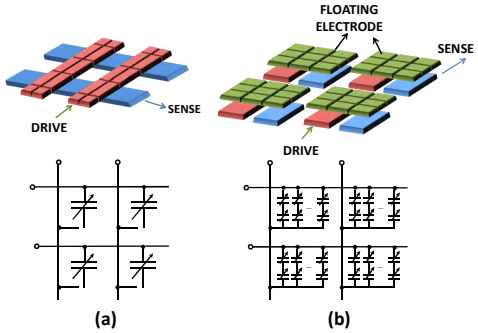

Figure 1. (a) Electrical failure due to the cracking of top electrodes during load application. (b) Formation of multiple floating electrodes due to cracking with total capacitance unchanged.

scheme of Fig. 1(b), a crack on the top layer breaks the total capacitance of the sensor into multiple smaller ones, but all of them are in parallel, thus the capacitance observed between the drive and sense lines remains unchanged. Floating electrodes were recently used to implement 8x8 array imagers that indirectly map pressure and shear [4]. These sensors fail to measure shear if the entire array is first normally loaded uniformly and then shear is applied.

A direct measurement of shear and pressure can be achieved using a conventional two-layer, 5-electrode capacitor configuration [5], where a single top (drive) electrode is separated from four overlapping bottom (sense) electrodes by an elastic dielectric. In this structure, the pressure P is obtained from the sum of all the four capacitors in the cell, while the shear vector $\vec{S} = (S_x, S_y)$ is extracted from the capacitance differences. Conventional 5-electrode cells do not use floating electrodes, and have a number of problems that make them unsuitable for array applications. The sensitivity to shear of these structures is also low. Nevertheless it will be shown in the sections below that the 5-electrode structure can be modified into a floating eight-electrode configuration that can be robust, more sensitive to shear and easily multiplexed. In this paper we present a high-density (676-sensor) floating-comb FTI that utilizes such modified sensing cell structure.

This project has been sponsored under DARPA contract W31P4Q-08-C-0253.

978-1-4577-1767-3/12/$26.00 ©2012 IEEE

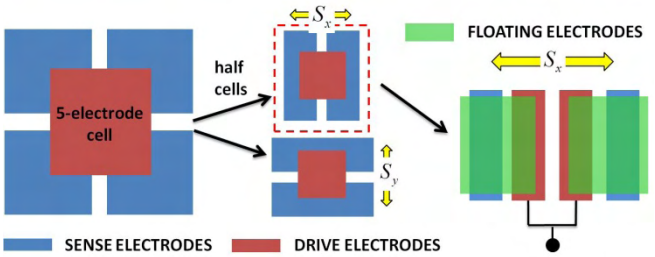

Figure 2. Evolution of a 5-electrode sense cell into a floating-electrode multi-fingered structure.

II. FTIs DESIGN WITH FLOATING ELECTRODES

In order to arrive to an easily addressable floating electrode cell, we modified the conventional 5-electrode cell as shown in Fig. 2. First the full cell is split into two orthogonal, three electrode half-cell sensors. Each half-cell can only measure shear in one direction. Next, drive electrodes are moved to the same plane as the sense electrodes, and for each half-cell we split the drive electrode and introduce two floating electrodes overlapping above both drive and sense lines. Note that the overlap on the two extremes of the drive electrodes is different such that when the floating electrode moves laterally one capacitor increases while the other decreases. The shear signal is extracted from the shifting overlap at the edge of the overlap. In order to magnify the shear sensitivity, we can shaped the overlap capacitor to maximize its edges by introducing the use of multi-fingered capacitors. The final multi-finger sensing cell is shown in Fig. 3. Capacitors 1, 2, 3 and 4 shown in Fig. 3 (c)-(i) can all measure pressure. Capacitors 1 and 2 can measure shear in Y direction and capacitors 3 and 4 can measure shear in X direction. When normal forces acting alone on the floating electrode, capacitance increases equally on all four capacitors. When shear in both directions is applied in addition to normal load as shown in Fig. 3(c)-(ii), capacitance in 1 decreases and capacitance in 2 increases (due to shear S_y represented by the arrow). In a similar way, capacitance in 3 will increase and capacitance in 4 decreases (due to a shear S_x). Hence, pressure can be measured by capacitance addition of 1 and 2 or 3 and 4 and shear in a given direction can be measured by capacitance difference of 1 and 2 or 3 and 4. Multiplexing of each full cell is explained in Fig. 4, which shows the four capacitors of a single cell without the deposition of floating electrodes. The four capacitances can be measured by individual excitation of each of the two red row lines (A, D) while reading on the vertical blue lines (B, C).

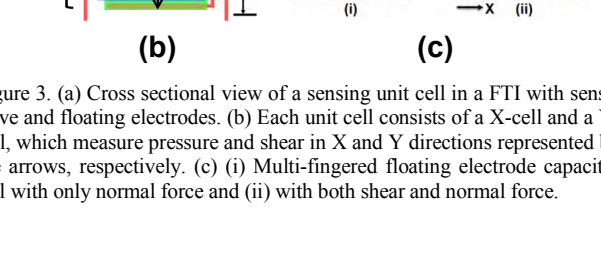

Figure 3. (a) Cross sectional view of a sensing unit cell in a FTI with sense, drive and floating electrodes. (b) Each unit cell consists of a X-cell and a Y-cell, which measure pressure and shear in X and Y directions represented by the arrows, respectively. (c) (i) Multi-fingered floating electrode capacitor cell with only normal force and (ii) with both shear and normal force.

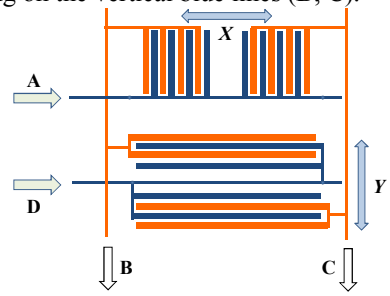

Figure 4. Multi-fingered cell illustrating the readout multiplexing scheme. The floating electrodes are removed for clarity.

The sensitivity of the multi-fingered floating electrode structure to pressure and shear are given by Eqs. (1)-(3), respectively,

$$S_P^F = \frac{1}{C}\frac{\partial C}{\partial P} = \frac{1}{E} \quad (1)$$

$$S_{SX}^F = \frac{1}{C}\frac{\partial C}{\partial S} = \frac{N_{fx}\cdot t}{2\cdot G\cdot w_f} \quad (2)$$

$$S_{SY}^F = \frac{1}{C}\frac{\partial C}{\partial S} = \frac{N_{fy}\cdot t}{G\cdot w_f} \quad (3)$$

where E and G are the elastic and shear modulus of the deformable dielectric, t is dielectric thickness, w_f is the finger width and N_{fx} and N_{fy} are the number of floating electrodes in the corresponding half cells. The shear sensitivity of this design thus increases linearly with the number of fingers.

When the cell structure shown in Fig. 3 is subject to both normal and shear forces, the (x, y, z) cell displacements in terms of capacitances are given by Eqs. (4)- (6),

$$x = \frac{d[(C_{AC}*C_{AB}^0)-(C_{AB}*C_{AC}^0)]}{(C_{AC}*C_{AB}^0)+(C_{AB}*C_{AC}^0)} \quad (4)$$

$$y = \frac{d[(C_{DC}*C_{DB}^0)-(C_{DB}*C_{DC}^0)]}{(C_{DC}*C_{DB}^0)+(C_{DB}*C_{DC}^0)} \quad (5)$$

$$z = \frac{t\cdot[2N_F(C_{DB}^0*C_{DC}^0)-(C_{AC}*C_{AB}^0)-(C_{AB}*C_{AC}^0)]}{(C_{AC}*C_{AB}^0)+(C_{AB}*C_{AC}^0)} = \frac{t\cdot[2N_F(C_{DB}^0*C_{DC}^0)-(C_{DC}*C_{DB}^0)-(C_{DB}*C_{DC}^0)]}{(C_{DC}*C_{DB}^0)+(C_{DB}*C_{DC}^0)} \quad (6)$$

where (C_{AB}^{o}, C_{AC}^{0}, C_{DB}^{0}, C_{DC}^{0}) are the cumulative of initial capacitances formed between the drive and floating electrodes and floating and sense electrodes connected in series as shown in Eqs. (7)-(8),

$$C_{AB}^{0} = \frac{C_{AF}^{0} * C_{FB}^{0}}{C_{AF}^{0} + C_{FB}^{0}}, \quad C_{AC}^{0} = \frac{C_{AF}^{0} * C_{FC}^{0}}{C_{AF}^{0} + C_{FC}^{0}} \tag{7}$$

$$C_{DB}^{0} = \frac{C_{DF}^{0} * C_{FB}^{0}}{C_{DF}^{0} + C_{FB}^{0}}, \quad C_{DC}^{0} = \frac{C_{DF}^{0} * C_{FC}^{0}}{C_{DF}^{0} + C_{FC}^{0}} \tag{8}$$

where (C_{AF}^{0}, C_{DF}^{0}) are the initial unstressed capacitances between drive and floating electrodes, and (C_{FB}^{0}, C_{FC}^{0}) are the initial unstressed capacitances between floating and sense electrodes.

III. FTI Fabrication

The FTIs with floating electrodes were fabricated using a combination of flexible printed circuit board (FPCB) techniques post-processed with microfabrication techniques for deposition of floating electrodes on flexible elastomeric dielectric material (PDMS). The use of FPCB substrates assures a high manufacturing yield and produces devices that can be cut into any dimensions with built-in connector cables. Fig. 5 shows a simplified process flow. A custom two-layer FPCB substrate was designed with the desired sense and drive line patterns for the FTI. The substrates were manufactured elsewhere (Uniflex Circuits, Ca) with the following process steps. First, a flexible 25µm Kapton base panel with 12µm copper is hard rolled with dry photoresist and patterned. After etching unwanted copper, drive and sense lines are formed. Another 25µm Kapton without any copper is adhered (using pressure and heat) to the previous flex substrate. Blind hole vias are then drilled through the second Kapton layer to connect all the drive electrodes in a row. A second layer of 12µm copper is adhered and patterned using dry photoresist. The second layer of copper is then covered by adhering a coverlay material (similar to Kapton film). One end of the FPCB is patterned to form a flexible printed cable (FPC) to match the connector from the readout circuitry. The manufactured FPCB substrates are next spin coated with a15µm thick PDMS film on the backside to form the elastic dielectric of the cells. We next deposit a 20nm Cr and 150nm gold films by e-beam evaporator. The films are next patterned to form the floating electrodes. The fabricated FTIs have a total of 2028 floating comb electrodes distributed over an area of about 49 cm^2. Fig. 6 shows a comparison of the fabricated FPCB before and after the deposition of the PDMS and floating electrodes.

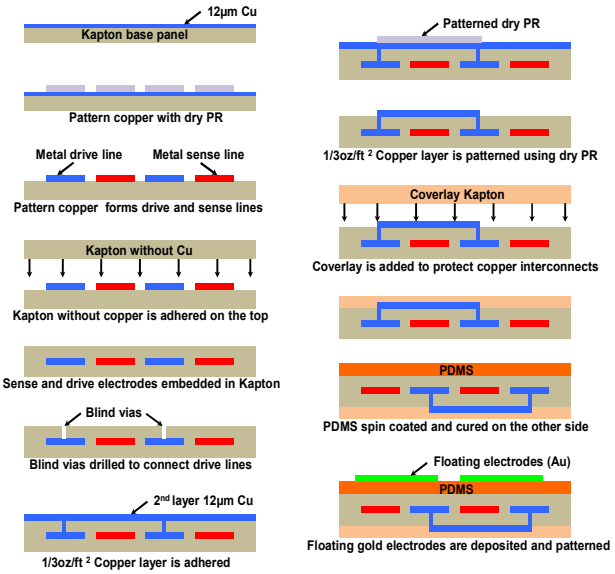

Figure 5. Process flow representing fabrication of FPCB with drive and sense lines. Last two steps depict in-house fabrication of the PDMS layer and gold floating electrodes over FPCB.

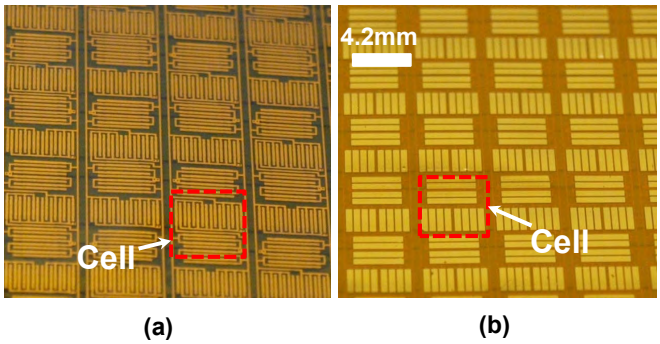

Figure 6. (a) FPCB substrate without floating metal layer. (b) After depositing PDMS and floating electrodes.

IV. Testing Results

After the fabrication, FTIs are characterized in a set of experiments with the FTIs integrated with a custom CMOS switched-capacitor circuit capable of measuring the capacitance of each comb cell (~0.5 pF) with a resolution of 12-bits in 10 ms producing frame rates as high as 100 Hz. The details of the circuitry are discussed elsewhere [6]. Fig. 7 shows the integration of FTI with the ASIC readout circuit board by using a low-profile flex cable connector. Testing can be categorized into three sections.

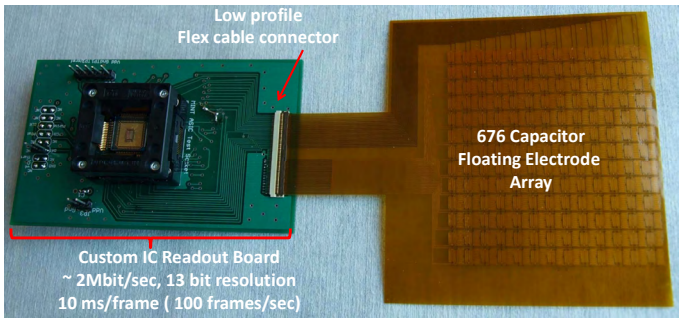

Figure 7. Flex imaging array integrated with customized ASIC readout circuit board.

a) Characterization of individual cell: Individual cells of the FTI are interrogated with pre-set values of normal force/shear applied on them and the corresponding voltage changes are recorded and plotted as shown in Fig. 8 (a) and Fig. 8 (b). The voltage change increased linearly for both increasing normal force and shear.

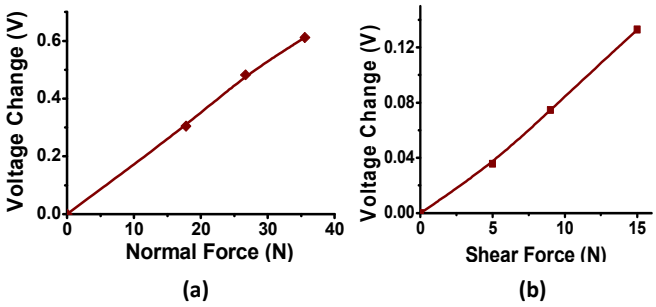

Figure 8. Graphs (a) and (b) represent change in voltage at different normal and shear forces exerted on an individual cell respectively.

b) Dynamic contour pressure mapping using FTI: In order to characterize dynamic pressure mapping using FTI, a softball was placed on top of it and an increasing normal force was then applied on top of the ball. As the pressure was increased, the contact area between the softball and FTI also increased, resulting in a change of the pressure contours as shown in Fig. 9.

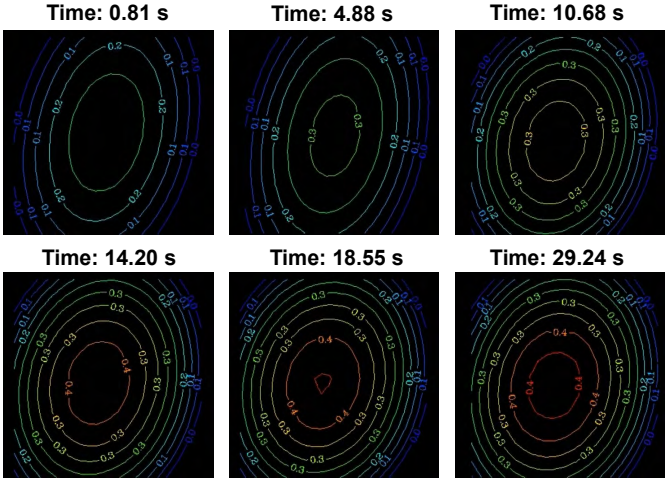

Figure 9. Dynamic pressure contour under increasing normal pressure.

c) Dynamic contour shear mapping using FTI: The dynamic contour shear mapping was performed in a similar way as the pressure mapping, but instead of applying the force right on the top, the softball was manually twisted, which generated the shear force between the softball bottom surface and FTI. The measured shear contours for different time intervals are shown in Figure 10.

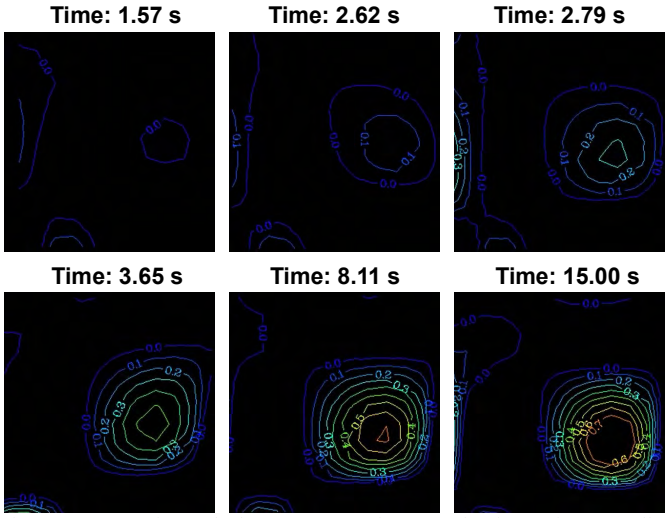

Figure 10. Experimental shear contour of FTI under increasing manully applied shear at different time intervals.

V. Conclusion

We successfully fabricated a 3-axis high-resolution flexible tactile imager system consisting of a new type of sensor cell formed using floating electrodes supported by an elastic layer on top of a FPCB substrate. Each sensing cell consists of multi-finger drive and sense electrodes on the FPCB and floating electrodes placed at an offset on a elastomeric dielectric material spin coated over the FPCB. The new cell design is easily multiplexed in large arrays. The fabricated FTI compactly packed 676 sense capacitors in about 49 cm^2.

References

[1] V. J. Lumelsky, M. S. Shur, and S. Wagner, "Sensitive skin," IEEE Sensors J., vol. 1, no. 1, pp. 41–51, Jun. 2001.

[2] R. A. Boie, "Capacitive impedance readout tactile image sensor," *Proc. 1984 IEEE International Conference on Robotics and Automation*, vol.1, no., pp. 370- 378, 1984.

[3] D. Johnston, Ping Zhang, J. Hollerbach and S. Jacobsen, "A full tactile sensing suite for dextrous robot hands and use in contact force control," *Proc. 1996 IEEE International Conference on Robotics and Automation*, vol.4, no., pp.3222-3227, 1996.

[4] M. Y. Cheng, C. L. Lin and Y. J. Yang, "Tactile and shear stress sensing array using capacitive mechanisms with floating electrodes," *Proc. IEEE MEMS*, vol., no., pp.228-231, 24-28 Jan. 2010.

[5] T. A. Chase and R. C. Luo, "A thin-film flexible capacitive tactile normal/shear force array sensor," *Proc. of the 1995 IEEE IECON 21st International Conference on Industrial Electronics, Control, and Instrumentation,* , vol.2, no., pp.1196-1201, 1995.

[6] M. Suster, et al, "Low-Interference Sensing Electronics For High-Resolution Error-Correcting Biomechanical Ground Reaction Sensor Cluster", Proc. IEEE Sensors, pp. 1020-1023, 2010.